

JOM 23586

Fluorenylrubidium · *N,N,N',N'',N''*-pentamethyldiethylenetriamine: a square-wave-like polymeric chain in the solid state

Daniele Hoffmann, Frank Hampel and Paul von Ragué Schleyer

Institut für Organische Chemie der Universität Erlangen-Nürnberg, Henkestraße 42, W-8520 Erlangen (Germany)

(Received December 3, 1992)

Abstract

The transmetallation of fluorenyllithium with $\text{RbO}^{\ddagger}\text{Bu}$ in THF yields fluorenylrubidium, which in the presence of PMDTA (*N,N,N',N'',N''*-pentamethyldiethylenetriamine) gives cube-shaped crystals of $[\text{C}_{13}\text{H}_9\text{Rb} \cdot \text{PMDTA}]_n$ (**1**). An X-ray diffraction study has shown that **1** adopts a “square-wave-like” polymeric chain structure, in which each rubidium cation is coordinated to two fluorenyl anions and one triamine ligand.

1. Introduction

The detailed nature of the interaction of alkali metal cations with π -delocalized carbanions depends on the size of both partner ions [1] and on the additional donor ligands, if these are present. As the bonding to highly delocalized carbanions is almost exclusively ionic [2], simple electrostatic point charge models [3] are often successful in predicting the locations of alkali metal gegenions. While small ions such as Li^+ are usually charge-localizing, larger ions (K^+ – Cs^+) often prefer multihapto interactions [4]. We have recently demonstrated this for $\text{Ph}_3\text{CM} \cdot \text{L}_n$ ($\text{M} = \text{K}, \text{Rb}, \text{Cs}$ and $\text{L}_n = \text{polar ligands}$) [5].

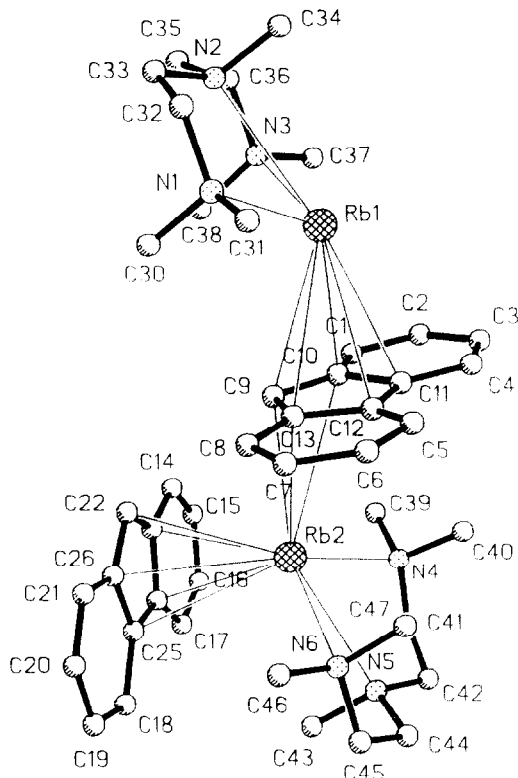
The fluorenyl “anion” also exemplifies the diversity of structures with alkali and alkaline earth metal cations. In solution, both contact ion pairs (CIPs) and/or solvent separated ion pairs (SSIPs) are known to exist [6]. The X-ray structures of several fluorenyllithium [7,8] and fluorenylsodium complexes [9], and those of fluorenylpotassium [10] and fluorenylbarium [11] reveal various coordination modes in the solid state. We have now investigated this system with the heavier alkali metals Rb and Cs. Do these alkali metal ions prefer an η^6 to an η^5 -coordination?

2. Results and discussion

The transmetallation of $\text{C}_{13}\text{H}_9\text{Li}$ with $\text{RbO}^{\ddagger}\text{Bu}$ in THF yielded $\text{C}_{13}\text{H}_9\text{Rb}$. Dark orange, cube-shaped crystals of $[\text{C}_{13}\text{H}_9\text{Rb} \cdot \text{PMDTA}]_n$ (**1**), suitable for X-ray structural analysis, were obtained after adding toluene and an excess of PMDTA. The molecular geometry of **1** is shown in Fig. 1. The compound crystallizes as a “square wave-like” polymeric chain (Fig. 2) with two $\text{C}_{13}\text{H}_9\text{Rb} \cdot \text{PMDTA}$ units per asymmetric unit. Selected geometrical information is given in Table 1, and fractional coordinates and anisotropic displacement parameters are listed in Table 2.

While there are two crystallographically distinct Rb^+ -cations, these have similar environments. Both $\text{Rb}(1)$ and $\text{Rb}(2)$ are coordinated η^5 and η^3 (Figs. 3a and 3b) to two fluorenyl anions and also to one PMDTA-ligand. The $\text{Rb}-\text{C}$ distances involved in the slightly asymmetrical η^5 -coordinations range between 321.9(14) and 341.1(15) pm for $\text{Rb}(1)$ and between 321.3(13) and 341.0(13) pm for $\text{Rb}(2)$. The $\text{Rb}(1)$ distance to the centre of the C(9)–C(13) ring is 309.6 pm; the $\text{Rb}(2)$ to ring centre distance [C(22)–C(26)] is 308.1 pm. Hence, the η^5 -coordination of the two Rb^+ -cations is very similar (cf. Table 1). The difference between the cations arises from their η^3 -interactions. While $\text{Rb}(1)$ coordinates in a benzylic fashion to C(21a), C(22a) and C(26a) [$\text{Rb}-\text{C}$: 315.6(13)–350.8(16) pm], $\text{Rb}(2)$ is located approximately above C(9) and inter-

Correspondence to: Prof. Dr. P.v.R. Schleyer.

Fig. 1. Molecular geometry of **1**.

acts in a more symmetric allylic fashion with C(9), C(10) and C(13) [Rb–C: 315.9(14)–352.4(15) pm] (*cf.* Fig. 3). The two cations interact in the same way with the triamine ligand. As expected, the longest Rb–N

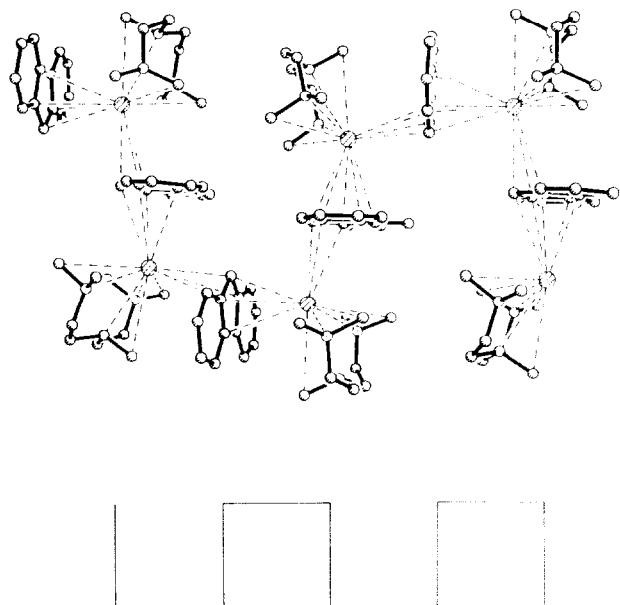
Fig. 2. Square-wave like polymeric array of **1** in the solid state. Bottom: schematic representation of a square wave.

TABLE 1. Selected bond lengths (pm) and angles (°)

<i>Bond lengths</i>			
Rb(1)–C(9)	333.1(15)	Rb(2)–C(22)	321.3(13)
Rb(1)–C(10)	321.9(14)	Rb(2)–C(23)	331.5(14)
Rb(1)–C(11)	326.8(13)	Rb(2)–C(24)	341.0(13)
Rb(1)–C(12)	337.6(15)	Rb(2)–C(25)	335.3(13)
Rb(1)–C(13)	341.1(15)	Rb(2)–C(26)	326.3(14)
Rb(1)–C(21a)	350.8(16)	Rb(2)–C(9)	315.9(14)
Rb(1)–C(26a)	322.7(14)	Rb(2)–C(10)	347.9(14)
Rb(1)–C(22a)	315.6(13)	Rb(2)–C(13)	352.4(15)
Rb(1)–N(1)	296.5(14)	Rb(2)–N(4)	303.2(13)
Rb(1)–N(2)	314.3(12)	Rb(2)–N(5)	309.9(12)
Rb(1)–N(3)	302.1(13)	Rb(2)–N(6)	302.4(12)
C(9)–C(10)	142.0(25)	C(22)–C(23)	140.5(24)
C(9)–C(13)	140.0(27)	C(22)–C(26)	139.8(22)
C(10)–C(11)	143.7(25)	C(23)–C(24)	144.0(20)
C(11)–C(12)	142.2(26)	C(24)–C(25)	143.3(23)
C(12)–C(13)	140.0(23)	C(25)–C(26)	146.1(19)
C(1)–C(2)	139.1(28)	C(14)–C(15)	132.4(30)
C(1)–C(10)	137.1(28)	C(14)–C(23)	140.4(26)
C(2)–C(3)	139.5(28)	C(15)–C(16)	140.1(26)
C(3)–C(4)	133.1(27)	C(16)–C(17)	136.3(27)
C(4)–C(11)	140.6(25)	C(17)–C(24)	140.8(23)
C(5)–C(6)	137.6(27)	C(18)–C(19)	138.7(23)
C(5)–C(12)	141.5(24)	C(18)–C(25)	142.6(21)
C(6)–C(7)	137.2(31)	C(19)–C(20)	141.4(24)
C(7)–C(8)	137.8(28)	C(20)–C(21)	134.8(23)
C(8)–C(13)	141.1(27)	C(21)–C(26)	138.4(25)
<i>Bond angles</i>			
N(1)–Rb(1)–N(2)	57.5(3)	N(4)–Rb(2)–N(5)	57.6(3)
N(2)–Rb(1)–N(3)	56.8(4)	N(5)–Rb(2)–N(6)	58.7(4)
C(10)–C(9)–C(13)	108.6(15)	C(23)–C(22)–C(26)	109.1(13)
C(9)–C(10)–C(11)	107.0(15)	C(22)–C(23)–C(24)	110.0(13)
C(10)–C(11)–C(12)	107.3(15)	C(23)–C(24)–C(25)	105.1(13)
C(11)–C(12)–C(13)	108.4(16)	C(24)–C(25)–C(26)	109.0(13)
C(9)–C(13)–C(12)	108.6(16)	C(22)–C(26)–C(25)	106.7(14)
C(8)–C(13)–C(12)	119.6(17)	C(14)–C(23)–C(24)	116.8(15)
C(7)–C(8)–C(13)	118.5(17)	C(15)–C(14)–C(23)	122.4(16)
C(6)–C(7)–C(8)	121.4(18)	C(14)–C(15)–C(16)	120.8(18)
C(5)–C(6)–C(7)	122.1(18)	C(15)–C(16)–C(17)	120.7(18)
C(6)–C(5)–C(12)	117.5(16)	C(16)–C(17)–C(24)	119.4(14)
C(5)–C(12)–C(13)	120.7(17)	C(17)–C(24)–C(23)	119.8(14)
C(1)–C(10)–C(11)	117.7(16)	C(21)–C(26)–C(25)	119.1(14)
C(2)–C(1)–C(10)	122.0(17)	C(20)–C(21)–C(26)	119.9(15)
C(1)–C(2)–C(3)	119.6(17)	C(19)–C(20)–C(21)	123.8(17)
C(2)–C(3)–C(4)	119.6(17)	C(18)–C(19)–C(20)	118.4(14)
C(3)–C(4)–C(11)	122.6(16)	C(19)–C(18)–C(25)	119.7(13)
C(4)–C(11)–C(10)	118.3(16)	C(18)–C(25)–C(26)	119.0(14)

distance is that to the central nitrogen [Rb(1)–N: 296.5(14)–314.3(12) pm and Rb(2)–N: 302.4(12)–309.9(12) pm].

The fluorenyl moieties (Fig. 1) are perpendicular (89.5° angle) to one another. The carbon skeletons are planar within experimental error and show the usual distortions [7–10]. The longer C–C distances (Table 1) in the five-membered ring compared to those in the six-membered rings may be considered in light of the computational results, which indicate that most of the negative charge is located in the central five-membered

ring. One of the annulated six-membered rings of each fluorenyl fragment exhibits an angle contraction at C(10) and C(23) [$C(14)C(23)C(24) = 116.8(15)^\circ$ and

TABLE 2. Atomic coordinates ($\times 10^4$) and equivalent isotropic displacement parameters ($\text{pm}^2 \times 10^{-1}$) for $[\text{C}_{13}\text{H}_9\text{Rb} \cdot \text{PMDTA}]_n$ (1)

	<i>x</i>	<i>y</i>	<i>z</i>	U_{eq}^{a}
Rb(1)	8465(1)	1313(1)	1864(1)	40(1)
C(1)	10801(9)	1174(12)	1472(11)	70(9)
C(2)	10887(10)	1967(15)	1118(8)	72(9)
C(3)	10757(9)	2783(12)	1431(10)	66(8)
C(4)	10545(8)	2794(11)	2062(9)	51(7)
C(5)	9928(8)	2406(10)	3585(9)	47(7)
C(6)	9721(10)	2026(14)	4176(10)	81(9)
C(7)	9738(11)	1118(15)	4280(9)	84(10)
C(8)	9929(9)	536(12)	3780(10)	65(8)
C(9)	10371(9)	486(11)	2576(10)	60(7)
C(10)	10537(9)	1163(11)	2106(9)	47(7)
C(11)	10424(8)	2008(12)	2429(9)	39(6)
C(12)	10170(9)	1824(10)	3079(10)	43(7)
C(13)	10137(9)	895(12)	3162(10)	46(7)
Rb(2)	12347(1)	419(1)	3220(1)	44(1)
C(14)	12542(12)	-1512(10)	1815(10)	72(9)
C(15)	13286(14)	-1466(11)	1578(10)	82(9)
C(16)	14070(12)	-1451(10)	2033(10)	70(9)
C(17)	14085(10)	-1506(9)	2728(9)	58(7)
C(18)	13574(8)	-1682(9)	4336(8)	50(7)
C(19)	13172(10)	-1802(10)	4911(8)	58(7)
C(20)	12260(11)	-1829(11)	4814(9)	67(8)
C(21)	11756(10)	-1780(10)	4191(9)	57(7)
C(22)	11804(9)	-1627(9)	2896(8)	53(7)
C(23)	12496(11)	-1582(9)	2523(8)	42(6)
C(24)	13303(9)	-1582(8)	2990(8)	36(6)
C(25)	13068(9)	-1642(8)	3665(8)	38(6)
C(26)	12128(9)	-1683(9)	3601(9)	44(6)
N(1)	7243(8)	487(9)	2688(6)	56(6)
N(2)	6820(8)	251(9)	1183(7)	49(6)
N(3)	8382(8)	270(9)	536(6)	55(6)
C(30)	7755(8)	-314(10)	2893(7)	61(7)
C(31)	7202(10)	1038(9)	3295(8)	89(9)
C(32)	6382(10)	261(11)	2330(8)	73(9)
C(33)	6342(9)	-219(10)	1669(9)	64(8)
C(34)	6377(9)	1068(10)	929(8)	83(9)
C(35)	6913(10)	-360(12)	628(8)	77(8)
C(36)	7534(11)	13(11)	158(8)	75(8)
C(37)	8841(9)	798(10)	56(7)	78(8)
C(38)	8900(9)	-505(10)	804(7)	74(8)
N(4)	13440(8)	1447(9)	2344(6)	54(6)
N(5)	14092(7)	1290(9)	3836(8)	57(6)
N(6)	12624(8)	1234(9)	4649(6)	57(6)
C(39)	13340(9)	1038(9)	1646(7)	78(8)
C(40)	13057(8)	2327(10)	2282(8)	80(8)
C(41)	14342(8)	1459(11)	2646(8)	72(8)
C(42)	14506(9)	1807(11)	3366(9)	73(8)
C(43)	14508(8)	422(10)	4002(7)	72(7)
C(44)	14089(9)	1781(12)	4478(9)	86(9)
C(45)	13536(10)	1387(13)	4956(8)	95(9)
C(46)	12162(10)	724(11)	5104(8)	110(10)
C(47)	12181(8)	2078(10)	4469(7)	71(8)

^a Equivalent isotropic U defined as one third of the trace of the orthogonalized U_{ij} tensor.

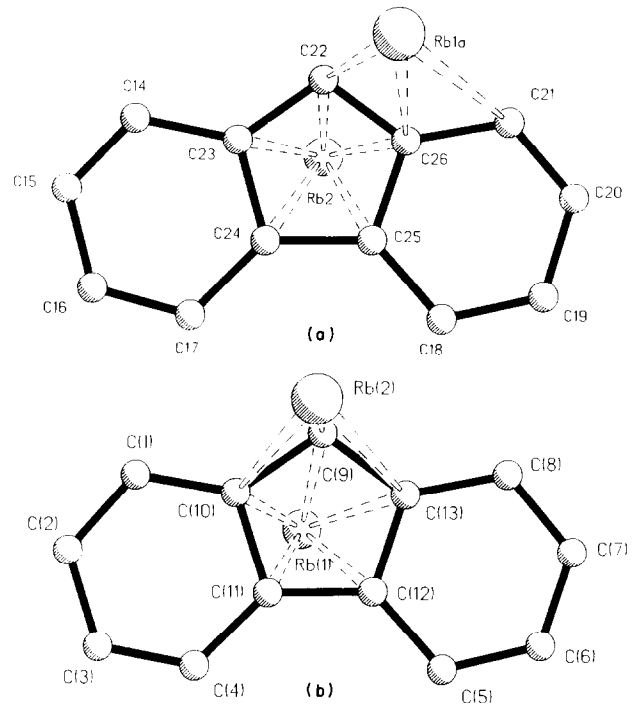


Fig. 3. The locations of Rb(1) and Rb(2) with respect to the two fluorenyl fragments.

$C(1)C(10)C(11) = 117.7(16)^\circ$. However, this quinonoid ring deformation is less pronounced than in the benzyl anion and related systems [12].

In monomeric $\text{C}_{13}\text{H}_9\text{Na} \cdot \text{PMDTA}$ [9] and in polymeric $\text{C}_{13}\text{H}_9\text{K} \cdot \text{TMEDA}$ [10], the alkali metal cations also are located above the five-membered rings. In the latter, the TMEDA acts as a bridging rather than a chelating ligand. This was attributed to the larger size of the K^+ cation, which for chelation of TMEDA was suggested to lead to an unfavourable, hypothetical $\text{N}-\text{K}-\text{N}$ angle of 58° [10]. However, in **1**, PMDTA does act as a tridentate ligand and the $\text{N}-\text{Rb}-\text{N}$ angles are $57.5(3)-58.7(4)^\circ$.

Structures of organorubidium compounds are scarce. The $\text{Rb}-\text{C}$ distances in **1** are in the range observed with other π -delocalized carbanions. These systems include $\text{Rb}_2\text{cot} \cdot \text{diglyme}$ ($\text{Rb}-\text{C}$: 310–343 pm) [13], N -rubidiocarbazole · PMDTA ($\text{Rb}-\text{C}$: 342–368 pm) [14], and $[\text{Ph}_3\text{CrB} \cdot \text{PMDTA}]_n$ ($\text{Rb}-\text{C}$: 335–364 pm) [5]. *Ab initio* calculations on unsolvated bridged allyl rubidium, as expected, predict somewhat shorter $\text{Rb}-\text{C}$ distances (302.5–305.2 pm) [15].

Crystals of fluorenylcesium were obtained as $[\text{C}_{13}\text{H}_9\text{Cs} \cdot \text{THF}]_n$ and as $[\text{C}_{13}\text{H}_9\text{Cs} \cdot \text{PMDTA}]_n$. In both cases, disorder in the carbanion moiety and in the triamine ligand, respectively, precluded refinement of the X-ray data. However, different coordination modes for the Cs^+ cation could be distinguished. In the

THF-complex, the Cs^+ is located above the six-membered ring, in the PMDTA-complex above the five-membered ring.

The potential energy surfaces in highly delocalized carbanions are shallow enough [2] to allow various coordination modes. That these depend strongly on the nature of the ligand [9] is also shown by MNDO studies on fluorenyllithium with various donor ligands, which predict energy differences of less than 6 kJ mol⁻¹ for the η^3 , η^5 and η^6 bonding modes [16]. Thus, even for Li^+ (which usually coordinates to the centres of highest charge), multihapto interactions (η^6) dominate in the solid state, if polar ligands are absent or are "weak" (Et_2O) [7c,d]. Monomeric, tetrameric and polymeric arrays with quite different cation locations were found for fluorenylsodium when PMDTA, TMPDA or TMEDA were used as polar ligands [9]. Hence, in **1**, the cation might change its preferred location from the five-membered to the six-membered ring if weaker, non-chelating, ligands such as Et_2O or THF were present.

Despite the availability of polar ligands (THF, PMDTA), the Rb^+ cation prefers to interact with a second fluorenyl fragment. That **1** crystallizes as a polymer rather than as a finite aggregate may be explained in terms of simple electrostatic models: the attractive Coulomb energy for an infinite chain of alternating unit charges is higher than for a finite cluster [17].

3. Experimental section

All manipulations were carried out under argon by use of Schlenk and needle septum techniques. Solvents were freshly distilled from Na/K alloy under argon. PMDTA was distilled from CaH_2 . $\text{RbO}^\ddagger\text{Bu}$ was prepared by reacting Rb metal with $^\ddagger\text{BuOH}$ in THF for one week. Removal of the THF *in vacuo* gives a white powder, which can be stored indefinitely under argon.

3.1. Preparation of **1**

To a solution of fluorene (781 mg, 4.7 mmol) in 8 ml of THF at -20°C were added 2.8 ml (4.5 mmol) of $^\ddagger\text{BuLi}$ (1.6 M solution in hexane). The dark orange solution was allowed to warm to room temperature and a solution of 752 mg (4.8 mmol) of $\text{RbO}^\ddagger\text{Bu}$ in 8 ml of THF was added, followed by 6.5 ml of toluene and 8.5 ml (39.7 mmol) of PMDTA. The solution was filtered and the filtrate stored at room temperature for two days. This afforded dark orange cube-shaped crystals of X-ray quality. Total yield 1.58 g (83%). Anal. Calcd. for $\text{C}_{22}\text{H}_{32}\text{N}_3\text{Rb}$: C, 62.32; H, 7.61; N, 9.91. Found: C, 62.39; H, 7.68; N, 9.94%. ^1H NMR (400 MHz, $d_8\text{-THF}$, $+26^\circ\text{C}$): δ 7.90 (2H, d, $J = 7.7$ Hz, H-4,5), 7.33 (2H, d, $J = 8.3$ Hz, H-1,8), 6.86 (2H, t, $J = 7.15$ Hz, H-2,7), 6.49 (2H, t, $J = 7.15$ Hz, H-3,6), 5.99 (1H, s, H-9); PMDTA-signals at δ 2.32 and 2.22 (4H, t, $J = 6.5$ Hz, N-CH₂), 2.06 (15H, s, N-CH₃). ^{13}C NMR (100.6 MHz, $d_8\text{-THF}$, $+26^\circ\text{C}$): δ 136.87 (C-10,13), 121.83 (C-11,12), 120.31 (C-2,7), 119.48 (C-4,5), 116.97 (C-1,8), 109.54 (C-3,6), 83.44 (C-9); PMDTA signals at δ 58.40 and 57.02 (N-CH₂), 45.78 (N-CH₃ terminal); 42.57 (N-CH₃ central).

Crystal structure determination ($T = 200 \pm 1$ K; Siemens R3m/V-diffractometer, crystals mounted in capillaries) for **1**: $M = 424.0$, monoclinic, space group $P2_1/c$, $a = 15.692(4)$, $b = 14.955(6)$, $c = 19.609(7)$ Å, $\beta = 99.11(3)^\circ$, $U = 4544(2)$ Å³, $D_c = 1.240$ g cm⁻³, $Z = 8$, $F(000) = 1776$, $\lambda = 0.71073$ Å (graphite monochromated Mo K α radiation). Data were collected on a specimen of $0.3 \times 0.4 \times 0.4$ mm³ using the ω -scan method ($3^\circ \leq 2\theta \leq 52^\circ$). Three standard reflections were measured every 100 reflections. From 8994 unique reflections 3238 with $I > 6.0\sigma(I)$ were used in the structure solution (direct methods) and subsequent structure refinement (SHELXTL-PLUS). $R = 0.0936$ and $wR = 0.0497$, GOF = 2.20.

Tables of atomic coordinates, bond lengths and angles, and thermal parameters have been deposited at the Cambridge Crystallographic Data Centre.

Acknowledgments

This work was supported by the Fonds der Chemischen Industrie and the Deutsche Forschungsgemeinschaft. We thank Thomas Sahiri for experimental assistance.

References

- 1 E.D. Jemmis and P.v.R Schleyer, *J. Am. Chem. Soc.*, **104** (1982) 4781.
- 2 C. Lambert, M. Kaupp, and P.v.R. Schleyer, *Organometallics*, **12** (1993) 853.
- 3 R.J. Bushby and H.L. Steel, *J. Chem. Soc., Perkin Trans. 2* (1990) 1143, 1155, 1169.
- 4 C. Schade and P.v.R. Schleyer, *Adv. Organomet. Chem.*, **27** (1987) 169.
- 5 D. Hoffmann, W. Bauer, P.v.R. Schleyer, U. Pieper and D. Stalke, *Organometallics*, **12** (1993) 1193.
- 6 (a) D. Hoffmann, W. Bauer and P.v.R. Schleyer, *J. Chem. Soc., Chem. Commun.*, (1990) 208; (b) J.B. Grutzner, J.M. Lawlor and L.M. Jackman, *J. Am. Chem. Soc.*, **94** (1972) 2306; (c) R.H. Cox, *J. Phys. Chem.*, **73** (1969) 2649; *J. Am. Chem. Soc.*, **93** (1971) 3297; (d) H.W. Vos, H.H. Blom, N.H. Velthorst and C. MacLean, *J. Chem. Soc., Perkin Trans. 2*, (1972) 635; (e) E. Edlund, *Org. Magn. Reson.*, **12** (1979) 661.
- 7 (a) J.J. Brooks, W. Rhine, and G.D. Stucky, *J. Am. Chem. Soc.*, **94** (1972) 7339. (b) M. Walczak and G.D. Stucky, *J. Organomet. Chem.*, **97** (1975) 313; (c) H.-J. Schmidt and D. Rewicki, *Acta Crystallogr., A40* (1984) C-293. (d) D. Bladauski and D. Rewicki, *Chem. Ber.*, **110** (1977) 3920.

- 8 (a) B. Becker, V. Enkelmann and K. Müllen, *Angew. Chem.*, **101** (1989) 501; *Angew. Chem., Int. Ed. Engl.*, **28** (1989) 458; (b) S. Buchholz, K. Harms, M. Marsch, W. Massa and G. Boche, *Angew. Chem.*, **101** (1989) 57; *Angew. Chem., Int. Ed. Engl.*, **28** (1989) 72.
- 9 S. Corbelin, J. Kopf and E. Weiss, *Chem. Ber.*, **124** (1991) 2417.
- 10 R. Zerger, W. Rhine and G.D. Stucky, *J. Am. Chem. Soc.*, **96** (1974) 5441.
- 11 G. Mösges, F. Hampel and P.v.R. Schleyer, *Organometallics*, **11** (1992) 1769.
- 12 (a) T. Maetzke and D. Seebach, *Helv. Chim. Acta*, **72** (1989) 624; (b) H. Hope and P.P. Power, *J. Am. Chem. Soc.*, **105** (1983) 5320;
- (c) D. Thoeness and E. Weiss, *Chem. Ber.*, **111** (1978) 3157; (d) U. Schümann, U. Behrens and E. Weiss, *Angew. Chem.*, **101** (1989) 481, *Angew. Chem., Int. Ed. Engl.*, **28** (1989) 476.
- 13 J.H. Noordik, H.M.L. Degens J.J. Mooji, *Acta Crystallogr., B* **31** (1975) 2144.
- 14 K. Gregory, *Ph.D. thesis*, Universität Erlangen-Nürnberg, 1991.
- 15 N.J.R. Hommes and P.v.R. Schleyer, *J. Organomet. Chem.*, **409** (1991) 307.
- 16 D. Hoffmann and P.v.R. Schleyer, unpublished results.
- 17 C. Lambert, P.v.R. Schleyer, M.G. Newton, P. Otto and P. Schreiner, *Z. Naturforsch. B*, **47** (1992) 869.